# Study of the Decay of $Tm^{168}$ to Levels in $Er^{168}$ Using Coincidence and Directional Correlation Techniques*

J. J. Reidy,†‡ E. G. Funk, and J. W. Mihelich
*University of Notre Dame, Notre Dame, Indiana*
(Received 9 September 1963)

The levels in $Er^{168}$ populated by electron capture of $Tm^{168}$ have been studied using scintillation spectrometers, gamma-gamma and electron-gamma coincidence measurements, and directional correlation techniques. This work leads to the following conclusions: the spin and parity of the 1543-keV level are verified as 3-; the 1280-keV transition is $E1(\leqslant 0.08\%M2)$; the 721-keV transition is $E1(\leqslant 0.05\%M2)$; and the 743-keV transition is $E2(\leqslant 2.4\%M1)$. The attenuation coefficient $\tilde{G}_2$ for the 1280–80-keV correlation was determined to be $0.77\pm0.19$ for a source consisting of a dilute aqueous solution of $TmCl_3$. The analysis of the results of the $Tm^{168}$ decay is compared with the predictions using various models. The ratios of reduced transition probabilities for transitions from the gamma vibrational band in $Er^{168}$ are analyzed and a band-mixing parameter $z=0.055$ is found.

## I. INTRODUCTION

THE excitation levels in even-even nuclei in the deformed region are characterized by a ground-state rotational band and a complicated set of levels which begin at energies above approximately 800 keV. Two models of the nucleus are widely used to describe these nuclear states: the unified model of Bohr and Mottelson[1] and the asymmetric rotator model first developed by Davydov and co-workers.[2] However, current models describing nuclear states have become more sophisticated. Attempts have recently been made[3–5] to interpret the states which are not quantitatively incorporated in the Bohr-Mottelson and Davydov models. Among such states are the negative parity states, usually described as octupole vibrations or intrinsic excitations.

It becomes increasingly important to have a better knowledge of the character of nuclear states. In particular, more precise information regarding the admixtures and relative intensities of the transitions depopulating the states and verification or establishment of many of the spins of these states is needed. Therefore, an investigation of the character of the states in the highly deformed nucleus $Er^{168}$ was undertaken. The results of this investigation will be compared with the results of similar recent studies.[6–8] The comparison of these results with theoretical calculations will be discussed and band-mixing parameters for the transitions from the gamma vibrational band in $Er^{168}$ will be presented.

It has been established that $_{69}Tm^{168}$ decays via electron capture to levels in $Er^{168}$ with a half-life of 87 days.[9] Jacob *et al.*[10] investigated the $Tm^{168}$ decay and presented a decay scheme and electron and photon intensities for most of the transitions. Half-life determinations[10–13] have been carried out for a few states in $Er^{168}$. The Coulomb excitation of the first excited state has been observed[14] and, recently, the possible Coulomb excitation of the second 2+ state (822 keV) has been reported.[15] The levels in $Er^{168}$ have also been studied by resonant neutron capture[9] in $Er^{167}$ and by the $Er^{167}(d,p)Er^{168}$ reaction.[16] In the present work, improved gamma-ray intensity measurements have been carried out. Some intensity ratios of gamma rays in composite peaks were determined from internal conversion electron-gamma ray coincidence data. Gamma-gamma directional correlation measurements were performed to establish the multipolarities of some of the transitions and to verify the originally postulated spins of the 1095-keV and the 1543-keV levels.

## II. PROCEDURE

Gamma-ray scintillation spectra were obtained using NaI (Tl) crystals ranging in size from $3\times3$ in. to 1 in. diam by 4 mm thick. A conventional fast-slow coincidence circuit with a resolving time ($2\tau$) of 0.10 $\mu$sec was employed with the scintillation spectrometers for the

* Work accomplished in part under contract with the U. S. Atomic Energy Commission.
† This work submitted as partial fulfillment for the degree of Doctor of Philosophy.
‡ Present address: Harrison M. Randall Laboratory, University of Michigan, Ann Arbor, Michigan.
[1] A. Bohr and B. R. Mottelson, Kgl. Danske Videnskab Selskab, Mat. Fys. Medd. **27**, No. 16 (1953).
[2] A. S. Davydov and G. F. Filippov, Nucl. Phys. **8**, 237 (1958).
[3] P. D. Lipas and J. P. Davidson, Nucl. Phys. **26**, 80 (1961).
[4] J. P. Davidson, Nucl. Phys. **33**, 664 (1962).
[5] C. J. Gallagher and V. G. Soloviev, Kgl. Danske Videnskab. Selskab, Mat. Fys. Skrifter **2**, No. 2 (1962).
[6] O. B. Nielsen in *Proceedings of the Rutherford Jubilee International Conference*, edited by J. E. Birks (Heywood and Company, Ltd., London 1962), p. 317.
[7] P. Gregors Hansen, O. B. Nielsen, and R. K. Sheline, Nucl. Phys. **12**, 389 (1959).
[8] G. T. Ewan, R. L. Graham, and J. S. Geiger, Nucl. Phys. **22**, 610 (1961).
[9] *Nuclear Data Sheets*, compiled by K. Way *et al.* (Printing and Publishing Office, National Acadamy of Sciences—National Research Council, Washington 25, D. C.), NRC 60-1-75.
[10] K. P. Jacob, J. W. Mihelich, B. Harmatz, and T. H. Handley, Phys. Rev. **117**, 1102 (1960).
[11] A. C. Li and A. Schwarzchild, Bull. Am. Phys. Soc. **7**, 359 (1962).
[12] E. Bodenstedt, H. J. Koerner, E. Gerdan, J. Radeloff, L. Mayer, K. Auerbach, J. Braunsfurth, and G. Mielken, Z. Physik **170**, 355 (1962).
[13] M. Birk, G. Goldring, and Y. Wolfson, Phys. Rev. **116**, 730 (1959).
[14] B. Elbek, M. C. Olsen, and O. Skilbreid, Nucl. Phys. **19**, 523 (1960).
[15] O. Nathan and V. I. Popov, Nucl. Phys. **21**, 631 (1960).
[16] R. A. Harlan and R. K. Sheline, Bull. Am. Phys. Soc. **7**, 317 (1962).

gamma-gamma and conversion electron-gamma coincidence measurements. The electron detector was a $\frac{1}{32}$-in.-thick Pilot $B$ scintillator. The output of the coincidence circuit was used to gate a multichannel analyzer.

An intermediate-image spectrometer (IIS) of the Slätis-Siegbahn type was used to gate internal-conversion electron peaks in some conversion electron-gamma ray coincidence measurements. The gamma rays were detected using a 1-×2-in. NaI (Tl) crystal (resolution approximately 10% for 661-keV gamma rays). A fast-slow coincidence circuit of resolving time 0.10 μsec was employed. The output of this circuit was used to gate a 256 channel analyzer. The IIS sources were made by separating the target material from the activity using the ion-exchange method.[17] The activity, which was in the form of the oxide, was dissolved in 6$N$ HCl and deposited on a thin Mylar film (1 mg/cm$^2$) which was attached to the Lucite source holder.

Directional correlation measurements were performed with a fast-slow coincidence circuit having a resolving time ($2\tau$) which was adjustable from 0.010 to 0.050 μsec. These resolving times insured a true to chance coincidence ratio of at least twenty to one for all correlations reported in this work. For most correlations this ratio was fifty to one. For energies above 500 keV, 2-×2-in. NaI (Tl) crystals were employed. A 1-×$\frac{1}{2}$-in. crystal was used for energies between 200 and 500 keV and a 1-in. diam by 4-mm-thick crystal for energies below 200 keV. The 2-×2-in. and 1-×$\frac{1}{2}$-in. crystals were shielded laterally with approximately 4 g/cm$^2$ of Pb. For correlations involving gamma rays of less than 100 keV, 4 g/cm$^2$ of Cu shielding was placed over all Pb shielding to minimize detection of Pb fluorescence radiation. The various frontal shields that were used are described later. The correlations were performed using an automatic directional correlation apparatus, and were run in the normal double quadrant sequence. Data were taken usually at five angles per quadrant but in some cases the counting rates were so small that data were taken only every 45°. The data were analyzed by the least-squares method as described by Rose.[18] The resulting coefficients were corrected for finite angular resolution using the results of Arns *et al.*[19] for the 2-×2-in. crystals and using the method described by Rose[18] for the other crystals.

## III. RESULTS AND CONCLUSIONS

The radioactive sources were made by proton irradiations of enriched $Er_2O_3$. The source was then allowed to age for about two months so the $Tm^{167}$ ($T_{1/2}$=9.6 days) fraction would decay sufficiently to give a relatively pure source of $Tm^{168}$ ($Tm^{167} \leq 5\%$).

### A. Gamma-Ray Intensity Measurements

Gamma-ray singles spectra obtained with a 3-×3-in. NaI (Tl) crystal are shown in Fig. 1. The source distance was 25 cm and no frontal absorber was used. The relative intensities of the prominent gamma rays were obtained by breaking apart a number of such spectra in the conventional way. Efficiency curves of Wolicki *et al.*,[20] peak-to-total ratios of Heath,[21] and escape peak intensity to total peak intensity ratios of Crouthamel[22] were used in the analysis. The resulting intensities are presented in column 2 of Table I. Relative $K$-conversion electron intensities of Jacob *et al.*[10] are presented in column 4 of Table I. It would have been ideal to normalize the gamma-ray intensities with respect to the intensity of the 80-keV gamma ray since this is the only gamma ray of known multipolarity[10] which is not part of a composite peak in the singles spectrum. However, the 80-keV peak height is only about three times higher than the Compton background and the exact shape of this background spectrum could not be determined.

A suitable normalization can be effected by requiring (1) the experimental internal conversion coefficient for the 198-keV transition to be at least as large as the theoretical $E1$ conversion coefficient, (2) the 185-keV transition to be $E2$ (as is evident from the work of Jacob *et al.*), and (3) consistency among the photon intensities in the 80-$L$ coincidence data of Table II (i.e., the 198-keV transition must be of sufficient intensity to account for the intensity of the 817-keV transition). A normalization which satisfies these requirements will result if the 448-keV transition is assigned a photon intensity of approximately 1400 units. This results in an experimental $K$-conversion coefficient indicating an $M1$ multipolarity for the 448-keV transition.

Conversion electron-gamma coincidence measurements were obtained by gating with the 80-$L$, 185-$L$, and 198-$K$ conversion electrons. The 80-$L$ conversion electrons were detected in a Pilot $B$ scintillator. The gamma-ray spectrum was obtained with a $1\frac{1}{2}$-×2-in. NaI (Tl) crystal (~7.5% resolution at 661 keV) at a source distance of 10 cm. The singles and coincidence spectra are shown in Figs. 2(a) and 2(b), respectively. The coincidence spectrum with the electron gate set above the 80-$L$ conversion electron peak is shown in Fig. 2(c). Figures 2(b) and 2(c) were normalized so the 1280-keV transition is of equal intensity in each. A point by point subtraction of these two curves was performed. The intensity of each transition in the resulting spectra is that part of the transition which is in coincidence with

[17] G. R. Choppin and R. J. Silva, Inorg. and Nucl. Chem. **3**, 153 (1956).
[18] M. E. Rose, Phys. Rev. **91**, 610 (1953).
[19] R. G. Arns, R. E. Sund, and M. L. Wiedenbeck (privately circulated report).
[20] E. A. Wolichi, R. Jastrow, and L. Brooks, Naval Research Laboratory Report NRL-4833, 1956 (unpublished); and S. H. Vegors, Jr., L. L. Marsden, and R. L. Heath, Atomic Energy Commission Research and Development Report IDO-16370 (unpublished).
[21] R. L. Heath, Phillips Petroleum Company, Atomic Energy Division (unpublished).
[22] *Applied Gamma-Ray Spectrometry*, edited by C. E. Crouthamel (Pergamon Press, Inc., New York, 1960).

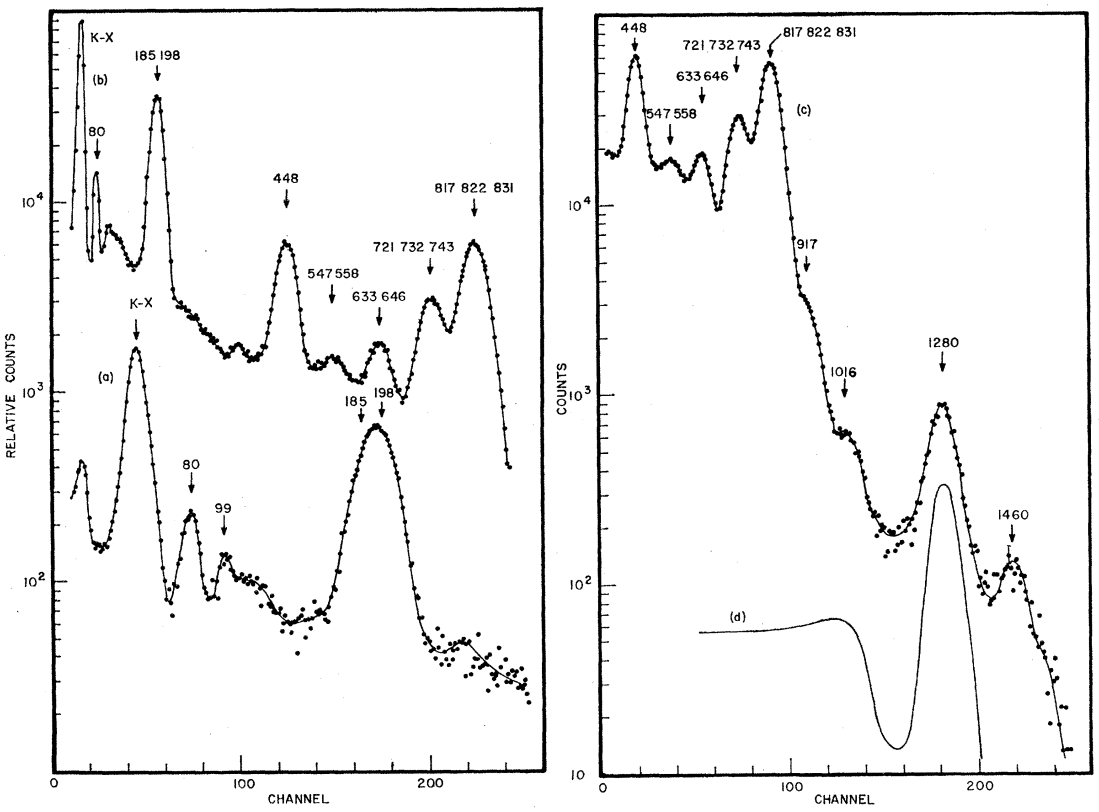


FIG. 1. Gamma-ray scintillation spectra for $Tm^{168}$ obtained with a 3-×3-in. NaI(Tl) detector at 25 cm. Curves (a), (b), and (c) show the spectrum from 15–250, 20–900, and 400–1500 keV, respectively. Curve (d) shows a 1280-keV contour ($Na^{22}$).

TABLE I. Intensity data for transitions in $Er^{168}$.

| Transition (keV) | Photon Intensity $N_\gamma$ | | $K$-Conversion Electron Intensity $N_e$ | Experimental Internal Conversion Coefficient $\alpha_K$ | Multiple Order | Total Intensity $N_\gamma(1+\alpha_T)$ |
|---|---|---|---|---|---|---|
| $K$ x-ray | 6820±700[a] | | | | | 6820 |
| 80 | 590±100 | | (1960)[b] | ($\alpha_L$=3.33) | $E2$ | 4400±25% |
| 99 | 180±90 | | | | | |
| 185 | 3970±400 | 1000[c] | 200 | | | 1330 |
| 198 | | 2970 | 140 | 4.5(−2) | $E1$ | 3150 |
| 273 | <100 | | 4 | >4.0(−2) | $E1+M2[M2]$ | |
| 448 | 1400 | | 58 | 4.1(−2) | $M1$ | 1460 |
| 547 | 250±75 | 250±100 | ~0.7 | 2.8(−3) | $E1$ | 250 |
| 558 | | | weak | | | |
| 633 | 750±150 | 770±100 | 5.7 | 7.4(−3) | $E2$ | 770 |
| 646 | | [140] 10 | ~0.4 | | [$E1$] $M2$ | |
| 721 | | 900[d] | 2.0 | | $E1$ | 900 |
| 732 | 2100±300 | 600 | 2.1 | 3.5(−3) | $E2$ | 600 |
| 743 | | 830[d] | 4.5 | | | |
| 817 | | 3350 | 14 | 4.2(−3) | $E2$ | 3350 |
| 822 | 4600±400 | 800[c] | 3.5 | | | |
| 831 | | <440 | 0.7 | >1.4(−3) | $E1$ and/or $M2$ | 440 |
| 917 | 210±30 | | 0.7 | 3.3(−3) | $E2$ | 210 |
| 1016 | 17±5 | | ~0.05 | ~2.9(−3) | $E1$? | |
| ~1085 | 10±4 | | | | | |
| ~1180 | 25 | | | | | |
| 1280 | 135±20 | | ~0.12 | ~8.9(−4) | $E1$ | 135 |
| ~1365 | 12 | | | | | |
| 1464 | 18±7 | | weak | | | |
| ~1525 | 15 | | | | | |

[a] 84% for $K$-capture; 16% for $K$-conversion.
[b] $L$-conversion electron intensity.
[c] Assumed $E2$ to obtain $N_\gamma$.
[d] $N_\gamma$ calculated from M. O. obtained using directional correlation results.

the 80-keV transition and not in coincidence with the 185-keV transition. Thus, all transitions feeding the 264-keV state are eliminated. However, this normalization does result in a greater number of 185-$K$ and 198-$K$ coincidences being subtracted from the coincidences obtained with 80-$L$ gate than is actually the case, so the intensities of those transitions also in coincidence with the 198-keV transition will be too low; since only $\sim 6\%$ of the 80-$L$ gate is due to the 198-$K$ conversion electron intensity, this effect will be small. The resulting relative intensities are presented in Table II. These intensity values have a statistical uncertainty of 20%.

The 185-$L$ and 198-$K$ conversion electrons were detected using the intermediate-image spectrometer. The gamma-ray singles spectrum is shown in Fig. 3(a). Figures 3(b) and 3(c) show the coincidence spectra resulting from gating with the 185-$L$ and 198-$K$ conversion electrons, respectively. The results are presented in Table II. The error in the intensities is 20%, except where noted. The 185-$L$ gate contained some 198-$L$ electrons ($\leq 10\%$) but the exact amount could not be determined. As a result, the intensity of the 831-keV transition given in column 2 of Table II is an upper limit only. The results of the coincidence data and the directional correlation measurements, which are presented below, are consistent with the decay scheme shown in Fig. 4.

TABLE II. Gamma-ray coincidence data for transitions in $Er^{168}$.

| Gate | Coincident Transition Energy (keV) | Photon Intensity $I_\gamma$ | Total Transition Intensity |
|---|---|---|---|
| 1280 $\gamma$ | $K$ x-ray | 915 | 915[a] |
| | 80 | 96 | 740[b] |
| | 185 | 555 | 720 |
| 80-$L$[c] | 185, 198 | ≥3100 1000 ≥2100 | |
| | 547 | 70±35 | |
| | 721, 743 | 1200 | |
| | 817 | 2900 | |
| | 917[d] | 210 | |
| | 1016 | 37±10 | |
| | 1464 | 17±7 | |
| 185-$L$ | 198 | 480±145 | |
| | 547, 558 | 250 | |
| | 640 | 1000 | |
| | 732 | 600 | |
| | 831 | 950 | |
| | 1050? | 49 | |
| | 1280[d] | 135 | |
| 198-$K$ | 633 | 118 | |
| | 817 | 510±50 | |

[a] 615 units for $K$-capture; 300 units for $K$-conversion.
[b] $\alpha_{total} = 6.7$.
[c] Part of transition intensity in coincidence with 80-keV transition and not in coincidence with 185-keV transition.
[d] Gamma rays normalized to the intensity of this transition given in Table I.

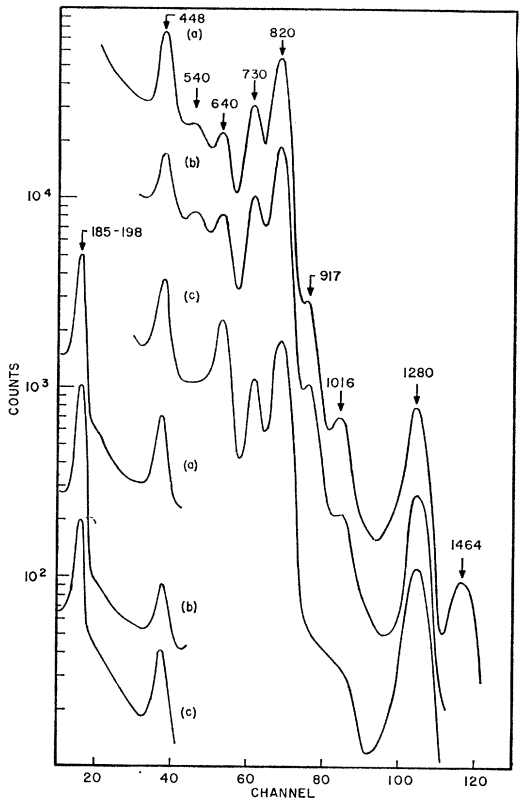


FIG. 2. Gamma-ray coincidence spectra obtained when gating electrons of ~80 keV (detected in a $\frac{1}{32}$-in.-thick Pilot $B$ scintillator). Curve (a) shows a singles spectrum from 150–1500 keV, (b) the coincidence spectrum with a gate set on the *80-L* internal conversion electron peak, and (c) the coincidence spectrum with the gate set on the region around 150 keV.

This is the decay scheme postulated by Jacob *et al.* with some minor changes, i.e., the log$ft$ values have been changed slightly and the 1095-keV level (spin value of 3 postulated by Jacob *et al.*) is now allowed the additional possible spin values of 2 or 4. This decay scheme is presented here as an aid in the discussion of the following analyses.

Since the 1280-keV photon intensity was used for normalization in some of the conversion electron-gamma coincidence analysis, a gamma-gamma coincidence was performed gating with the 1280-keV peak. This measurement checked the possibility that another transition with an approximate energy of 1280 keV may proceed directly to the 80-keV level. The singles spectrum and coincidence spectrum (chances subtracted) for a 1280-keV gate are shown in Figs. 5(a) and 5(b), respectively. The results, labeled 1280 $\gamma$, are presented in Table II. It is evident that the total intensity of the 80- and 185-keV transitions are nearly equal. Considering the statistical uncertainty one may conclude that the intensity of any "1280"-keV transition feeding the 80-keV state directly must be less than 20% of the intensity of the 1280-keV transition feeding the 264-keV state.

TABLE III. Results of directional correlation measurements on cascades in $Er^{168}$.

| Correlation (keV-keV) | Experimental Results $W(\theta)=1+A_2P_2+A_4P_4$ $A_2$ | $A_4$ | $W(\theta)=1+A_2P_2$ $A_2$ | Sequences Possible | Preferred | Remarks | Gates (Fig. 6) |
|---|---|---|---|---|---|---|---|
| 1280–80 | −0.107±0.021 | 0.039±0.030 | −0.094±0.018 | | | | *E,F* |
| 1280–185 | −0.140±0.023 | 0.019±0.033 | −0.132±0.020 | 3(*D*,*Q*)4(*Q*)2<br>5(*D*,*Q*)4(*Q*)2 | 3-4-2 | $-0.027\leq\delta\leq0.027$<br>$Q\leq0.08\%$ | *E,G* |
| 831–185 | 0.001±0.019 | 0.006±0.023 | | | | | *D,H* |
| 721–822 | −0.067±0.013 | 0.018±0.021 | −0.061±0.011 | *J*(*D*,*Q*)2(*Q*)0 where *J* has the values 1–5 | 3-2-0 | $-0.22\leq\delta\leq0.012$ | *A,C* |
| 721–743 | 0.000±0.014 | −0.008±0.023 | | | | | *A,A* |
| 721–743 (corrected for 721–822 interference) | 0.008±0.017 | −0.011±0.029 | | | 3(*D*)2(*D*,*Q*)2 | $\delta>6.3, Q\geq97.6\%$<br>$[-0.54\leq\delta\leq0.27$<br>$6.8\%\leq Q\leq22.5\%]$ | |
| 198–817 | −0.019±0.021 | 0.000±0.025 | −0.019±0.019 | 2(*D*,*Q*)3(*D*,*Q*)2<br>3(*D*,*Q*)3(*D*,*Q*)2<br>4(*D*,*Q*)3(*D*,*Q*)2 | | | *J,B* |

## B. Directional Correlation Measurements

Directional correlations were carried out on the following gamma-ray cascades: 1280–80, 1280–185, 831–185, 721–822, 721–743, 448–198, 198–817, and 198–185 keV. The correlation source was a dilute solution of $TmCl_3$ dissolved in 6*N* HCl. The source strength was approximately 4$\mu$ Ci.

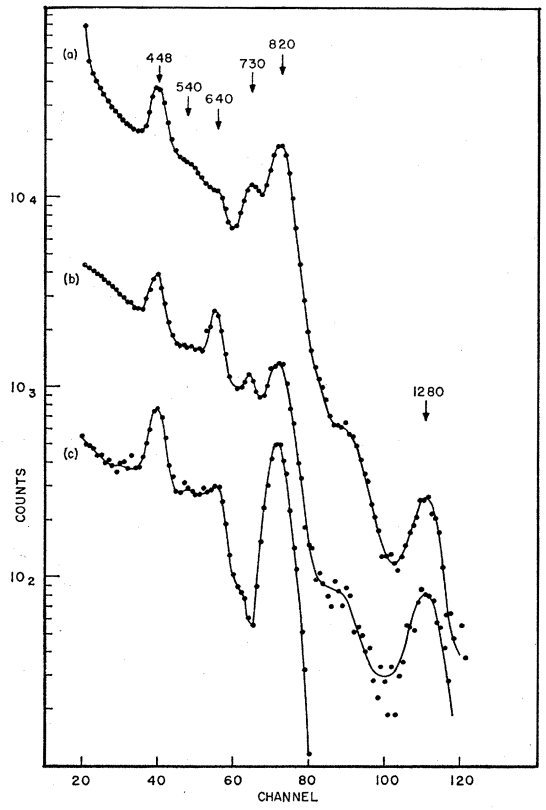


FIG. 3. Gamma-ray coincidence spectra obtained when gating 185-*L* (curve b) and 198-*K* (curve c) internal conversion electrons. The electrons were detected using the intermediate-image spectrometer. Curve (a) shows a gamma-ray singles spectrum.

The 448–198-keV correlation gave an isotropic distribution as might be expected since the 198-keV transition depopulates a relatively long-lived metastable state. The statistical error for the 198–185-keV correlation was too large to permit a reasonable analysis. This large error results from the relatively high Compton background coincidence rate compared to the 198–185-keV coincidence rate. This result might be expected since the 198-keV transition is also in coincidence with the Compton background of the very intense 817-keV transition. The results of the remaining correlations are presented in Table III. No corrections for interfering cascades have been made except where noted and only statistical errors were included in the analysis. The gamma-ray singles spectra and gate regions for the various correlations are shown in Fig. 6. The letters designating the various gates correspond to the letters presented in the last column of Table III. For Figs. 6(a) and 6(b) the source distance was 7 cm and the frontal shielding was 2 g/cm² of Pb and 2 g/cm² of Cu. The spectrum in Fig. 6(c) was obtained with a source distance of 2.7 cm and 500 mg/cm² of Cu frontal shielding. The source distance in Fig. 6(d) was 7 cm and the frontal shielding was 980 mg/cm² of Cu.

### *1280–185 and 721–822 keV correlations*

There should be no interference in the 1280–185-keV correlation due to other cascades. From the level scheme it is evident that the 1280–185-keV cascade is a *J*-4-2 sequence where *J* denotes the spin of the 1543-keV level. The 4+ assignment for the 264-keV state and the *E2* assignment to the 185-keV transition have been discussed by Jacob *et al.* and are the most likely assignments. In addition, the internal conversion coefficient data presented in Table II indicates that the 1280-keV transition has a predominent *E1* character. Thus, the 1280–185-keV correlation data should be compatible with a *J*(*D*,*Q*) 4 (*Q*) 2 sequence. Only values of $J=3$ or $J=5$ satisfy this interpretation.

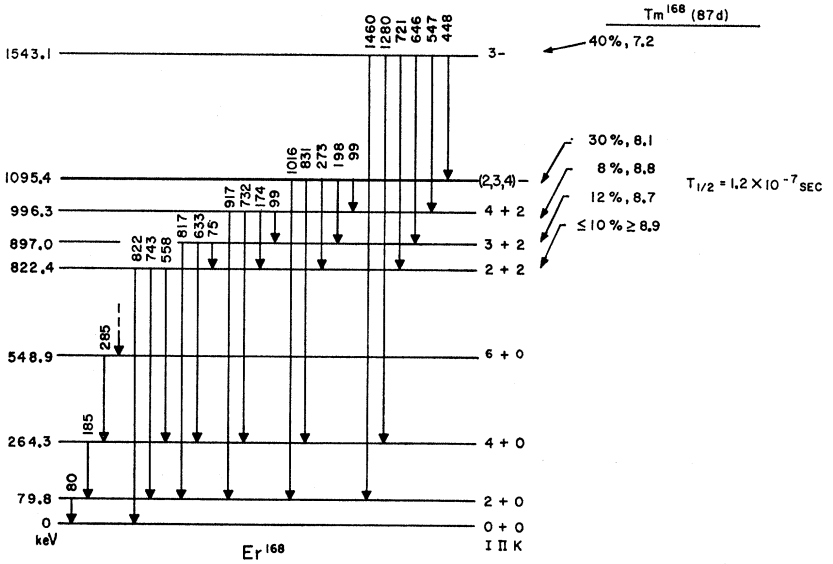


FIG. 4. Decay scheme of $Tm^{168}$.

The 721–822-keV correlation should also be free from interfering correlations. The Coulomb excitation of the 822-keV state has been reported[15] and, according to Jacob *et al.*, the 822-keV transition proceeds from this 2+ state to the 0+ ground state so the 721–822-keV cascade should have a $J$-2-0 spin sequence. $J$ denotes the spin of the 1543-keV state. The correlation data are compatible with all feasible values of $J$. A 5-2-0 sequence requires an admixture of $M4(M4\sim15\%)$, but this possibility seems highly unlikely since the 721-keV transition competes with the 448-keV $M1$ transition and, furthermore, the half-life ($T_{1/2}\leq 8\times10^{-10}$ sec)[13] of the 1543-keV state is too short to be consistent with an $M4$ admixture of this intensity. Since the 721- and 1280-keV transitions depopulate the 1543-keV level, the 721–822 and 1280–185-keV cascades must have the same initial spin. Only a spin of 3 for the 1543-keV state is consistent with both the 1280–185 and 721–822-keV correlation data. Thus, the 1280–185-keV correlation data must be compatible with the $3(D,Q)\ 4(Q)\ 2$ sequence. In Fig. 7 the theoretical values of $A_2$ and $A_4$ for this sequence are plotted versus $Q$, the quadrupole content of the initial transition. It is evident that the experimental values of $A_2$ and $A_4$, which are represented by the error flags, are consistent only with a value of $Q\leq0.08\%$. Thus, the 1280-keV transition is $E1+M2(M2\leq0.08\%)$. Since the 1280-keV transition is of $E1$ character and feeds the 264-keV (4+) state, the parity of the 1543-keV state must be negative. As a result, the spin and parity assignments of 3− for the 1543-keV state which were postulated by Jacob *et al.* are verified.

One now expects the 721–822-keV correlation data to be compatible with a $3(D,Q)\ 2(Q)0$ sequence. The experimental values of $A_2$ and $A_4$ are only consistent with a value of $Q\leq0.05\%$. Since the 721-keV transition proceeds from the negative parity 1543-keV state to the positive parity 822-keV state, this transition must be $E1+M2(M2\leq0.05\%)$. The 721–822-keV correlation data are shown in Fig. 8. The solid curve is the least-squares curve corrected for finite geometry and the dashed curve shows the theoretical $3(D)2(Q)0$ correlation function. The points represent the experimental

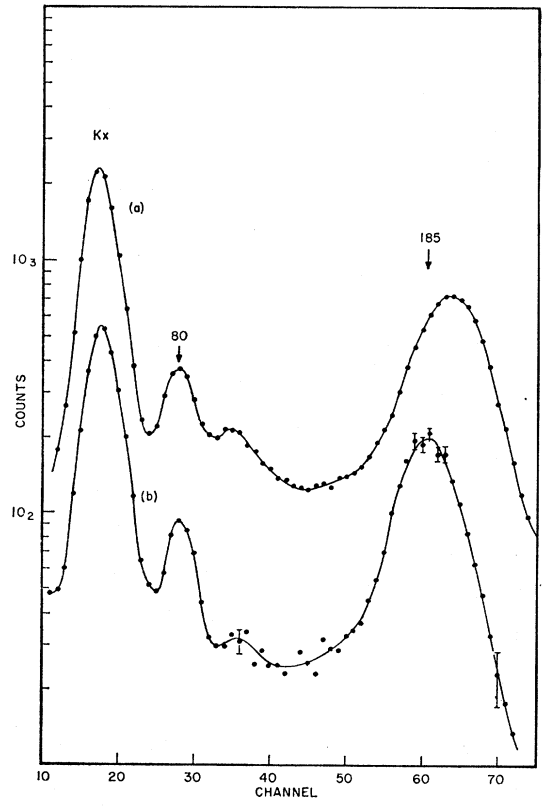


FIG. 5. Gamma-ray spectrum in coincidence with the 1280-keV gamma transition. Curve (a) shows the singles spectrum and curve (b) shows the coincidence spectrum (corrected for chances).

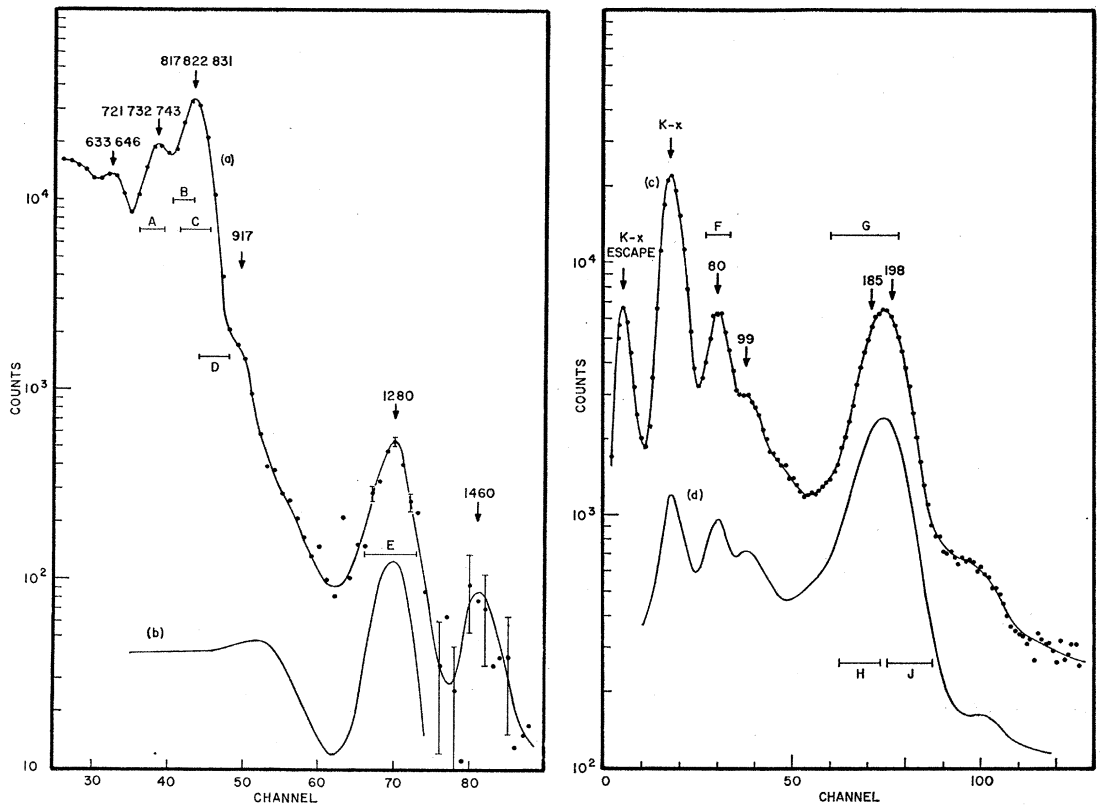


FIG. 6. Gamma-ray spectra and gates used for directional correlation measurements. Curve (a) shows a spectrum and gates ($A$-$E$) using a 2-×2-in. NaI crystal; (b) a 1280-keV contour ($Na^{22}$) for the same geometry as (a); (c) a spectrum and gates ($F$,$G$) using a 4-mm ×1-in. NaI crystal; and (d) a spectrum and gates ($H$,$J$) using a 1-×½-in. crystal.

data with the errors being the root-mean-square statistical error only.

### *721–743-keV correlation*

The 721–743-keV correlation was performed to determine the multipole mixture in the 743-keV transition. The differential discriminators in both detector arrangements were set to accept both the 721- and 743-keV energy intervals [position A shown in Fig. 6(a)]. This correlation has to be corrected for the interfering 721–822-keV correlation due to the 822-keV Compton distribution in the composite 721–743-keV gates. This correction was carried out in the following manner.

One detector arrangement which accepted the energy region $A$ (Fig. 6) was set at 90° with respect to the second detector arrangement which accepted the energy region $C$. The number of coincidence events per unit time was recorded. Since the 721–822-keV correlation function is known, the coincidence rate as a function of angle could be calculated. The ratio of the 822-keV transition intensity in gate $A$ compared to the 822-keV Compton intensity in gate $C$ was determined. Using this ratio and the 721–822-keV angular coincidence rate calculated above, the 721–822-keV coincidence rate was determined, where gate $A$ was used for both detector arrangements. This latter coincidence rate was subtracted, angle by angle, from the coincidence rate obtained in the experimental 721–743-keV correlation. This correction amounted to about a 10% change in the number of counts per angle. From the results of the 721–822-keV correlation one concludes that the 721-keV transition is essentially pure dipole. Furthermore, from the decay scheme one finds that the 743-keV transition proceeds from the 822-keV (2+) state to the 80-keV (2+) state. Thus, the 721–743-keV correlation is fitted to a $3(D)$ $2(D,Q)2$ sequence. In Fig. 9 the theoretical values of $A_2$ are plotted versus $Q$ for a $3(D)$ $2(D,Q)$ 2 sequence. The error flag represents the experimental $A_2$ coefficient. From this figure and the fact that the 743-keV transition proceeds between states of like parity it follows that the 743-keV transition is $M1+E2(6.8\% \leq E2 \leq 22.5\%$ or $E2 \geq 97.6\%)$. However, if the 743-keV transition is $M1+E2(7\text{–}23\%\ E2)$ then using the intensity data of Table I one finds the photon intensity of the 743-keV transition to be 450–460 units. This requires the 732-keV transition to have a photon intensity of 850 units. In this case, the 732-keV transition would be $E1+M2$, which is not consistent with the decay scheme where the 996-keV state is assigned positive parity. Also, a photon intensity of 850 units for the 732-keV transition is inconsistent with the coincidence measurements presented in Table II. We conclude that the 743-keV transition is

$E2+M1(M1\leq 2.4\%)$. From Table I it follows that the 732-keV transition is predominantly $E2$.

### *198–817-keV correlation*

This correlation was run to help determine the spin of the 1095-keV level. The interfering 831–185-keV cascade probably contributed less than 3% of the total coincidences and is neglected. The results of this correlation are inconclusive. If one assumes that the 817-keV transition is pure $E2$ and proceeds from a 3+ to a 2+ state, then the $2(D,Q)\ 3(Q)2$ and $4(D,Q)\ 3(Q)2$ sequences are preferred. The $3(D,Q)\ 3(Q)2$ sequence requires an $M2$ admixture of at least 18% in the 198-keV transition whereas the limit on this admixture is less than 2% as determined from the experimental $K$-conversion coefficient (Table I). However, an $M1$ admixture of approximately 1.5% in the 817-keV transition does allow a $3(D)3(D,Q)2$ sequence to be compatible with the results of the 198–817-keV correlation.

### *1280–80-keV correlation*

This correlation was performed to determine the time average attenuation of this correlation due to the mean-life of the 80-keV level. The correlation is due to a $3(D,Q)4(Q)2(Q)0$ sequence and should be identical to a $3(D,Q)4(Q)2$ sequence. Since the 1280–185-keV cascade is a $3(D,Q)4(Q)2$ sequence and is presumably unattenuated, the time average attenuation coefficients $\bar{G}_k$ for the 1280–80-keV correlation can be obtained by taking the ratio of the respective coefficients in the 1280–80- and 1280–185-keV correlations. For a liquid source of $TmCl_3$ dissolved in $6N$ HCl one finds that $\bar{G}_2=0.765\pm0.196$ and $\bar{G}_4=2.05\pm3.60$. Bodenstedt *et al.*[12] have found this correlation to be slightly attenuated for a liquid source of $Tm(NO_3)_3$ dissolved in $3N$ $HNO_3$. However, they were able to measure the differential angular correlation as a function of delay time and found $G_2=e^{-\lambda_2 t}$ where $\lambda_2=(5.8\pm2.9)\times10^7$ $sec^{-1}$. This time-dependent attenuation coefficient could not be determined in the present work due to the relatively large resolving time of our coincidence circuit.

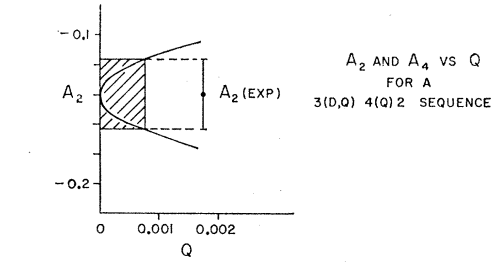


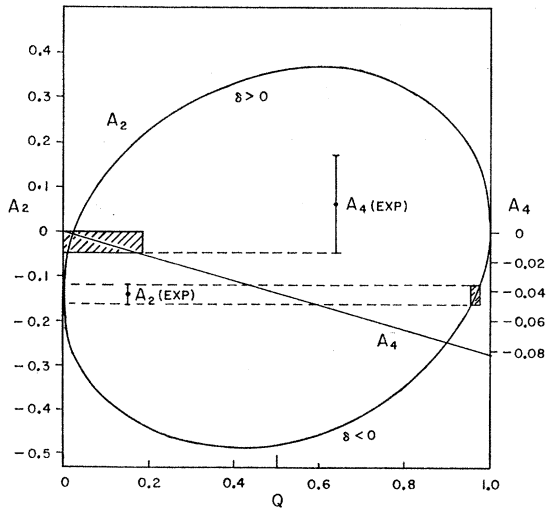


FIG. 7. Theoretical values of $A_2$ and $A_4$ plotted versus $Q$ (quadrupole content) for a 3 $(D,Q)$ 4 $(Q)$ 2 sequence. The experimental values of the coefficients for the 1280–185-keV correlation and the values of $Q$ consistent with these coefficients are shown on the graph.

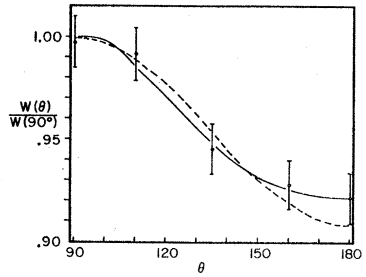


FIG. 8. Directional correlation data for the 721–822-keV correlation. The solid line is the least-squares fitted curve, and the dashed line the theoretical curve for a $3(D)\ 2(Q)\ 0$ sequence.

## C. Conclusions

The preceding analysis brings out certain features of the various energy levels. These features and additional conclusions are presented below for each of the levels.

### *1543-keV state*

The spin and parity of this level, as postulated by Jacob *et al.*,[10] have been verified as $3^-$. The transitions depopulating this state are predominantly dipole. The 1280-, 721-, and 448-keV transitions are essentially pure dipole and the 1464- and 547-keV transitions are most probably dipole. The 646-keV transition could be $E1$ and/or $M2$. The theoretical and experimental reduced transition probability (RTP) ratios for transitions from this level are shown in Table IV. The theoretical ratios are the predictions of Alaga *et al.*[23] No ratios are presented for the 1280- and 1464-keV transitions since these transitions are $K$-hindered if $K>1$ for the 1543-keV state. The experimental ratio of the value $B(E1)$ for the 646-keV transition $(3\rightarrow 3)$ to the value of $B(E1)$ for the 721-keV transition $(3\rightarrow 2)$ is obtained assuming that the 646-keV transition is pure $E1$ and is, therefore, the largest possible experimental ratio. This ratio is consistent with $K=3$ for the 1543-keV state. The experimental ratio of the value $B(E1)$ for the 547-keV transi-

[23] G. Alaga, K. Alder, A. Bohr, and B. R. Mottelson, Kgl. Danske Videnskab. Selskab, Mat. Fys. Medd. 29, No. 9 (1955).

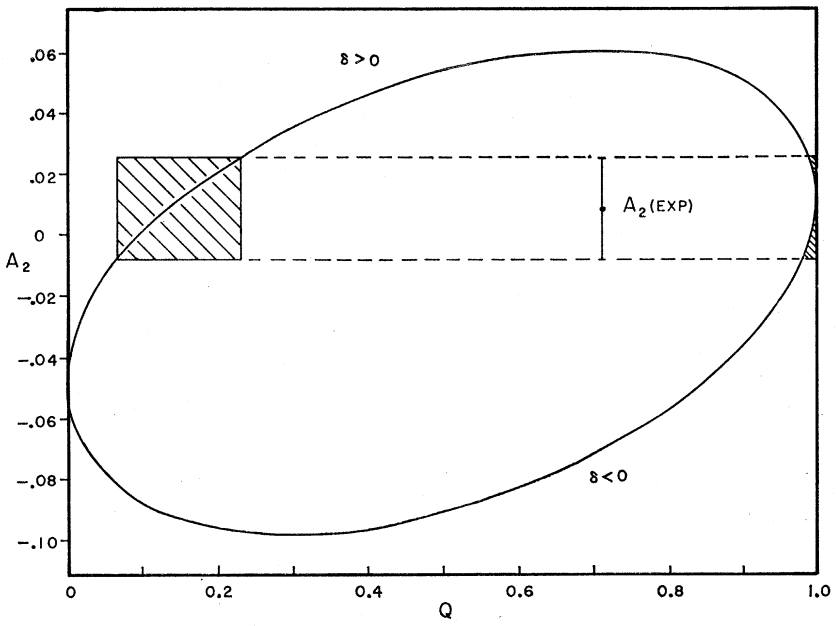


FIG. 9. Theoretical values of $A_2$ plotted versus $Q$ for a 3($D$) 2($D$,$Q$) 2 sequence. The experimental value of $A_2$ for the 721–743-keV correlation and the range of allowable $Q$ values are shown.

tion to the value of $B(E1)$ for the 721-keV transition is also maximal since the 547-keV transition is assumed to be pure $E1$ in this calculation. However, due to uncertainties in the electron and photon intensities for the 547-keV transition, it is possible that this transition is mixed. In this case the experimental ratio would be smaller and a $K=3$ assignment would be preferred. Thus, the most probable $K$ value for the 1543-keV state is $K=3$ although the data are only in fair agreement, at best, with this assignment.

### *1095-keV state*

Very little can be positively stated about this metastable state due to the uncertainties in the multipole assignments for the 831- and 1016-keV transitions. The

TABLE IV. Ratios of reduced transition probabilities for de-excitation of levels in Er.[168]

| Proposed $K$ $I\pi$ | Initial state (keV) | Final states ($K$, $I\pi$) | Assumed multipolarity | Reduced Transition probability ratios | Theoretical RTP ratios |
|---|---|---|---|---|---|
| 1 3−[a] | 1543 | (2,2+),(2,3+),(2,4+) | $E1$ | 1/≤0.22/≤0.63 | 1/8.8/11.3 |
| 2 | | | | | 1/1.4/1.8 |
| 3 | | | | | 1/0.35/0.05 |
| 1 2− | 1095 | (2,2+),(2,3+) | $E1$ | 0.013/1 | 0.5/1 |
| 2 | | | | | 2.0/1 |
| 1 3− | | (2,2+),(2,3+) | $E1$ | 0.013/1 | 0.11/1 |
| 2 | | | | | 0.71/1 |
| 3 | | | | | 2.86/1 |
| 0 2− | | (0,2+),(0,4+) | $M2$ | 0.13/1[c] | 0.56/1 |
| 1 | | | | | 0.3/1 |
| 2 | | | | | 19.8/1 |
| 0 3− | | (0,2+),(0,4+) | $E1$ | 0.2/1[d] | 0.75/1 |
| 1 | | | | | 1.3/1 |
| 0 3− | | (0,2+),(0,4+) | $M2$ | 0.14/1[c] | |
| 1 | | | | | 0.4/1 |
| 2 | | | | | 2.5/1 |
| 0 4− | | (0,2+),(0,4+) | $M2$ | 0.14/1[c] | 1.1/1 |
| 1 | | | | | 12.2/1 |
| 2 | | | | | 0.34/1 |
| 2 4+[b] | 996 | (0,2+),(0,4+) | $E2$ | 0.12/1 | 0.34/1 |
| 2 3+[b] | 897 | (0,2+),(0,4+) | $E2$ | 1.2/1 | 2.5/1 |
| 2 2+[b] | 822 | (0,2+),(0,4+) | $E2$ | 4.8/1[e] | 20.0/1 |
| | | (0,2+),(0,0+) | $E2$ | 0.55/1 | 0.7/1 |

[a] $I\pi$ are firm.
[b] $K$, $I\pi$ are firm.
[c] Both transitions are assumed to be pure quadrupole; photon intensity calculated from $K$-conversion electron intensity assuming pure $M2$.
[d] Both transitions are assumed to be pure dipole; photon intensity calculated from $K$ conversion electron intensity assuming pure $E1$.
[e] Upper limit of 0.5 set on electron intensity of 558-keV transition; photon intensity then calculated assuming 558 is pure $E2$.

spin assignment can be 2, 3, or 4 but the parity is certainly negative. Jacob *et al.* postulated a spin and parity assignment of 3− for this state.

### *822(2+)-, 897(3+)-, and 966(4+)-keV states*

The transitions from these levels to the ground-state rotational band exhibit a predominant $E2$ character which supports the gamma-band interpretation of Jacob *et al.* On the basis of this interpretation the theoretical and experimental ratios of RTP's for transitions from these levels are given in Table IV. The discrepancy between the experimental and theoretical ratios is consistent with the results generally obtained for transitions from the gamma vibrational band.[6–8] This point will be discussed later.

Log $ft$ values for the decay of $Tm^{168}$ to the various levels in $Er^{168}$ are presented in Table V. The log $ft$ values are calculated assuming three different values for $Q_{ec}$, the total energy available for electron capture. Cameron[24] and Seeger[25] predict 1634 and 2050 keV, respectively, for $Q_{ec}$. Since $Q_{ec}$ could not be determined in the present work, both possibilities are considered. The case where $Q_{ec}$ is the average of these two predicted values (1842 keV )is also presented to demonstrate the change in the log $ft$ values as one increases $Q_{ec}$ from the value of Cameron to the value of Seeger. These log $ft$ values will be discussed later.

## IV. DISCUSSION

The preceding results bring out some interesting aspects of the decay scheme of $Er^{168}$. The comparative lifetimes[26] of transitions de-exciting the negative parity levels at 1543 and 1095 keV are presented in Table VI. The $E1$ transitions depopulating the 1095-keV state are considerably retarded in comparison with the single particle estimates.[27] In the case of the 1543-keV level, the transitions proceeding to the $K=0$ ground-state band (1464 and 1280 keV) are retarded to a greater extent than the transitions to the $K=2$ gamma vibrational band. This might be indicative of $K$-hindrance of these transitions, and thereby help support the $K=3$ assignment for the 1543-keV state.

The log $ft$ values presented in Table V are difficult to interpret since $Q_{ec}$ is unknown. However, these results would be in fair agreement with the calculations of Gallagher and Soloviev[5] (denoted GS). Gallagher and Soloviev have interpreted the 1543-keV state as resulting from the coupling of two-quasiparticle Nilsson proton states and the 1095-keV state as resulting from the coupling of two-quasiparticle Nilsson neutron states. GS have assigned $3+,3(I\pi,K)$ to the $Tm^{168}$ ground state and 3−,3 to both the 1543- and 1095-keV states. The states in the gamma vibrational band and ground-state rotational band retain their usual collective character from Bohr-Mottelson theory. In the GS theory, these assignments require the electron-capture decay of $Tm^{168}$ to the gamma vibrational band to be totally forbidden. This forbiddenness would be consistent with the large experimental log $ft$ values for decay to these states. GS further predict that the log $ft$ values for decay to the negative parity states should be similar; if $Q_{ec}\sim 2000$ keV, the experimental log $ft$ values may be similar. It is possible to assign other $K$ values to the negative parity states in the GS theory, but the experimental data do not support any of the other possible assignments. The 1543-keV state might also be tentatively interpreted as the base state of a vibrational band using the Bohr-Mottelson (BM) or the asymmetric rotor models. However, the 1095-keV state cannot be interpreted in such a manner. The relatively long half-life of this state ($T_{1/2}=1.2\times10^{-7}$ sec) indicates that it is probably an intrinsic state due to some type of particle or quasiparticle excitation.

TABLE V. Log $ft$ values for electron-capture decay of $Tm^{168}$ to levels in $Er^{168}$.

| Level (keV) | Feeding % | Log $ft$ $Q_{ec}$[a]=1643 keV | 1841 keV | 2050 keV |
|---|---|---|---|---|
| 1543(3−) | 40 | 6.1 | 7.2 | 7.7 |
| 1095 | 30 | 7.9 | 8.1 | 8.3 |
| 996(4+) | 8 | 8.7 | 8.9 | 9.1 |
| 897(3+) | 12 | 8.5 | 8.7 | 8.9 |
| 822(2+) | 10 | 8.7 | 8.9 | 9.0 |

[a] For the meaning of the various values for $Q_{ec}$, see the text.

TABLE VI. Comparative lifetimes for transitions depopulating the 1543- and 1096-keV levels in $Er^{168}$.

| Energy keV | Transition Multiple Order | Comparative Lifetimes[a] $E1$ $(-14.2)^b$ | M1 $(-13.6)^b$ | M2 $(-8.1)^b$ |
|---|---|---|---|---|
| | 1543-keV level ($T_{1/2}\leq 8\times10^{-10}$ sec)[c] | | | |
| 1464 | $E1$ | $\leq -4.8$ | | |
| 1280 | $E1$ | $\leq -5.8$ | | |
| 721 | $E1$ | $\leq -7.4$ | | |
| 646 | $E1$ or $M2$ | $\leq -7.7$[d] | | $\leq -7.9$[e] |
| 547 | ($E1$) | $\leq -8.2$[d] | | |
| 448 | $M1$ | | $\leq -9.7$ | |
| | 1095-keV level ($T_{1/2}=1.2\times10^{-7}$ sec) | | | |
| 1016 | $E1$ and/or $M2$ | $-2.7$[d] | | $-2.7$[e] |
| 831 | $E1$ and/or $M2$ | $-4.6$[d] | | $-3.7$[e] |
| 273 | $E1$ and/or $M2$ | $-6.2$[d] | | $-5.1$[e] |
| 198 | $E1$ | $-7.3$ | | |

[a] See Ref. 26.
[b] Theoretical values (see Ref. 27).
[c] Upper limit of measured half-life (see Ref. 12).
[d] Transition is assumed to be pure dipole; photon intensity calculated from $K$-conversion electron intensity.
[e] Transition is assumed to be pure quadrupole; photon intensity calculated from $K$-conversion electron intensity.

[24] A. G. W. Cameron, Atomic Energy of Canada Limited Report AECL-433, 1957 (unpublished).
[25] P. A. Seeger, Nucl. Phys. **25**, 1 (1961).
[26] M. Goldhaber and A. W. Sunyar, in *Beta- and Gamma-Ray Spectroscopy*, edited by K. Siegbahn (North-Holland Publishing Company, Amsterdam, 1955), Chap. XVI.
[27] S. A. Moszkowski, in *Beta- and Gamma-Ray Spectroscopy*, edited by K. Siegbahn (North-Holland Publishing Company, Amsterdam, 1955), Chap. XIII.

TABLE VII. Theoretical ratios of reduced transition probabilities for transitions from the 822-, 897-, and 996-keV states.

| | Band mixing | | | | | | | | |
|---|---|---|---|---|---|---|---|---|---|
| | $z=0.00$ | 0.03 | 0.04 | 0.05 | 0.06 | 0.07 | Belyak and Zaikin[a] | Davydov and Filippov[b] | Exp. |
| 822-keV level (2+) | | | | | | | | | |
| $\frac{B(E2;22\rightarrow 00)}{B(E2;22\rightarrow 20)}$ | 0.70 | 0.59 | 0.55 | 0.52 | 0.50 | 0.47 | 0.51 | 0.46 | 0.55 |
| $\frac{B(E2;22\rightarrow 20)}{B(E2;22\rightarrow 40)}$ | 20.0 | 14.3 | 12.5 | 11.5 | 10.5 | 9.1 | 10.0 | | >4.8 |
| 897-keV level (3+) | | | | | | | | | |
| $\frac{B(E2;32\rightarrow 20)}{B(E2;32\rightarrow 40)}$ | 2.5 | 1.65 | 1.5 | 1.3 | 1.2 | 1.07 | 1.32 | 1.1 | 1.2 |
| 996-keV level (4+) | | | | | | | | | |
| $\frac{B(E2;42\rightarrow 20)}{B(E2;42\rightarrow 40)}$ | 0.34 | 0.22 | 0.19 | 0.16 | 0.13 | 0.11 | | 0.11 | 0.12 |

[a] See Ref. 28.
[b] See Refs. 2 and 29.

The discrepancy between the theoretical and experimental reduced transition probability ratios (Table IV) for transitions from the gamma vibrational band may be resolved by considering a possible rotation-vibration coupling between the $K=0$ ground-state band and the $K=2$ gamma vibrational band. Such a coupling can cause a considerable change in the intensity ratios due to the large transition probability for transitions between states in a rotational band.[7] The effect of mixing is taken into account by introducing a band-mixing parameter $z$ and a function $f(I_i,I_f,z)$ so that[7]

$$B_{\text{exp}}(E2;I_i2\rightarrow I_f0)=B_{\text{theor}}(E2;I_i2\rightarrow I_f0)f(I_i,I_f,z)$$
$$=\text{const.}(I_i2\ 2\text{-}2|I_i\ 2I_f0)^2f(I_i,I_f,z).$$

$B_{\text{exp}}$ denotes the experimental RTP, $B_{\text{theor}}$ is the theoretical RTP according to Alaga *et al.*,[23] and $I_i$ and $I_f$ are the spins of the initial and final states, respectively. The form of the function $f(I_i,I_f,z)$ is presented in Ref. 7. Obviously, a value of $z$ can be determined for each observed branching ratio. However, if deviations from the uncorrected theoretical branching ratios actually are due to the rotation-vibration interaction (i.e., if this interpretation of the mixing parameter $z$ is valid) a single value of $z(=z_0)$ should apply for all transition rates from one band to another for a given nucleus.[7] In this case the theoretical corrected reduced transition probability $B_{\text{corr}}$ for each transition is given by

$$B_{\text{corr}}(E2,I_i2\rightarrow I_f0)=B_{\text{theor}}(E2;I_i2\rightarrow I_f0)f(I_i,I_f,z_0).$$

Table VII presents the experimental ratios and the corrected theoretical ratios of RTP's for values of the band-mixing parameter $z$ ranging from 0.03 to 0.07. One value, $z=0.04$, is most consistent with the ratio $B(E2;22\rightarrow 00)/B(E2;22\rightarrow 20)$ whereas a second value, $z=0.06$, is most consistent with the other ratios. However, the possible errors in the experimental RTP ratios presented in Table VII would enable one to choose a single value of $z$ which could best explain all the data. This value of $z$ is approximately 0.055 and is roughly equal to the mixing parameters determined for other nuclei in this region.[6-8] Columns 8 and 9 of Table VII give the ratios predicted by Belyak and Zaikin[28] (denoted BZ) and Davydov and co-workers,[2,29] respectively. BZ also consider the interaction of the ground state rotational band with the gamma vibrational band using the BM model of the nucleus. Our data are in good agreement with their results. Unlike the method of mixing parameters discussed above, the ratio of RTP's predicted by BZ depend only on the parameter $\mu=E(2,2)/E(2,0)$ where $E(I,K)$ denotes the energy of the state $(I,K)$. From the calculations presented in Table VII it is evident that the results of BZ are similar to those results using a mixing parameter $z=0.05$. The ratios of Davydov were calculated using the predicted value for $\gamma_0$ of 12.3° and are approximately the same as those obtained from band-mixing with $z=0.06$. This value of $\gamma_0$ was obtained from the ratio of the energies of the second and first 2+ states. Actually, a value of $\gamma_{\text{exp}}=11.9°$ gives better agreement between the experimental and theoretical ratios. This difference in the values of the angle as obtained from the energy ratio and from electromagnetic transition probabilities is usually present and may be due to a rotation-vibration interaction. For nu-

[28] V. I. Belyak and D. A. Zaikin, Izv. Akad. Nauk. SSSR (Ser. Fiz.) **25**, 1163 (1961); Nucl. Phys. **30**, 442 (1962).
[29] A. S. Davydov and V. S. Rostovsky, Nucl. Phys. **12**, 58 (1959).

TABLE VIII. Comparison of experimental and theoretical ratios of reduced transition probabilities for transitions de-exciting the gamma vibrational bands in $Er^{166}$ and $Er^{168}$.

| | $Er^{166}$ | | | | | $Er^{168}$ | | | | |
|---|---|---|---|---|---|---|---|---|---|---|
| | Exp.[a] | Band mixing $z=0.045$ | Davydov and Filippov $\gamma_0=12.9°$, $\gamma_{exp}=10°$ | | Belyak and Zaikin $\mu=9.77$ | Exp.[b] | Band mixing $z=0.055$ | Davydov and Filippov $\gamma_0=12.3°$, $\gamma_{exp}=11.9°$ | | Belyak and Zaikin $\mu=10.3$ |
| $\frac{B(22\rightarrow 00)}{B(22\rightarrow 20)}$ | 0.56 | 0.54 | 0.44 | 0.53 | 0.50 | 0.55 | 0.51 | 0.46 | 0.49 | 0.51 |
| $\frac{B(32\rightarrow 20)}{B(32\rightarrow 40)}$ | 1.35 | 1.4 | 1.0 | 1.42 | 1.28 | 1.2 | 1.25 | 1.1 | 1.2 | 1.32 |
| $\frac{B(42\rightarrow 20)}{B(42\rightarrow 40)}$ | 0.17 | 0.17 | 0.10 | 0.18 | | 0.12 | 0.14 | 0.11 | 0.12 | |

[a] Obtained from Ref. 31.
[b] Obtained from this work.

clei approaching the transition region (e.g., $Os^{186,188,190}$) one finds that $\gamma_{exp}$ is sometimes less than $0.75\gamma_0$.[30]

It is interesting to compare the results of this analysis with the results of a similar analysis for the transitions depopulating the gamma vibrational band in $Er^{166}$. This comparison is presented in Table VIII. The experimental data for the transitions in $Er^{166}$ are taken from Ref.[31]. A value of 0.045 for $z$ is most consistent with these data. All the ratios presented for $Er^{166}$ are quite consistent with the single value of $z$. Since the energy difference between the $K=2$ and $K=0$ bands is less in $Er^{166}$ than in $Er^{168}$, one would expect the mixing in $Er^{166}$ to be greater than in $Er^{168}$. However, the opposite is true (see Table VIII).

It is possible to explain this apparent discrepancy by noting that the possible error in the experimental RTP ratios (of the order of 20%) would allow one to choose a smaller mixing parameter for the $Er^{166}$ case than for the $Er^{168}$.

From the preceding discussion it is evident that the ratio of RTP's for transitions from the gamma vibrational band in the two deformed nuclei $Er^{166}$ and $Er^{168}$ are compatible with theoretical estimates only if some type of rotation-vibration interaction is considered. These results are consistent with the results of other investigators. This rotation-vibration interaction may even become so large that it may be difficult (or meaningless) to assign a definite $K$ quantum number to certain states. Even though the asymmetric rotor model does not include $K$ as a quantum number, a rotation-vibration interaction must still be introduced in order to obtain agreement with the experimental data. Gallagher and Soloviev have used a quasiparticle treatment to classify many states in deformed even-even nuclei but no theoretical estimates of the ratio of RTP's were presented. However, even in this treatment one might expect a coupling treatment to be necessary since the ground-state band and gamma vibrational band retain their usual collective character.

*Note added in proof.* Nielsen[6] has concluded that mixing of the gamma-vibrational and ground-state bands is not sufficient to explain the observed deviations from the $I(I+1)$ rule for the energies of the ground state rotational spectra. Recently Greenberg *et al.*[32] have shown that the indicated mixing of the beta-vibrational and ground-state bands can account for the remainder (90%) of the energy perturbation of the 4+ state in the ground-state band.

## ACKNOWLEDGMENTS

The authors wish to thank Dr. F. J. Schima for many helpful discussions and C. W. Siedel for programming parts of the analysis for the IBM-1620 computer. One of us (J.J.R.) wishes to thank the National Science Foundation for their support through a Summer Teaching Fellowship.

[30] G. T. Emery, W. R. Kane, M. McKeown, M. L. Perlman, and G. Scharff-Goldhaber, in *Proceedings of the Conference on Electromagnetic Lifetimes and Properties of Nuclear States, Gatlinburg, Tennessee, 1961.* Nuclear Science Series Report No. 37 (National Academy of Sciences—National Research Council, Publication 974, Washington 25, D. C., 1962).

[31] B. Harmatz, T. H. Handley, and J. W. Mihelich, Phys. Rev. **123**, 1758 (1961).

[32] J. S. Greenberg, G. G. Seaman, E. V. Bishop, and D. A. Bromley, Phys. Rev. Letters **11**, 211 (1963).